



Contents lists available at ScienceDirect

Chinese Chemical Letters

journal homepage: [www.elsevier.com/locate/ccllet](http://www.elsevier.com/locate/ccllet)

## Versatile catalytic membranes anchored with metal-nitrogen based metal oxides for ultrafast Fenton-like oxidation



Qingbai Tian<sup>a</sup>, BingLiang Yu<sup>a</sup>, Zhihao Li<sup>b,\*</sup>, Wei Hong<sup>c,\*</sup>, Qian Li<sup>a</sup>, Xing Xu<sup>a,\*</sup>

<sup>a</sup> Shandong Key Laboratory of Water Pollution Control and Resource Reuse, School of Environmental Science and Engineering, Shandong University, Qingdao 266237, China

<sup>b</sup> Henan water Conservancy Survey design Research Co., Ltd., Zhengzhou 450000, China

<sup>c</sup> Shandong Resources and Environment Construction Group Co., Ltd., Ji'nan 250100, China

### ARTICLE INFO

#### Article history:

Received 26 April 2024

Revised 4 July 2024

Accepted 6 August 2024

Available online 10 August 2024

#### Keywords:

Peroxymonosulfate

Catalytic membranes

Metal oxides

Fenton-like reaction

Ceramic membrane

### ABSTRACT

Although the powder Fenton-like catalysts have exhibited high catalytic performances towards pollutant degradation, they cannot be directly used for Fenton-like industrialization considering the problems of loss and recovery. Therefore, the membrane fixation of catalyst is an important step to realize the actual application of Fenton-like catalysts. In this work, an efficient catalyst was developed with Co-N<sub>x</sub> configuration facily reconstructed on the surface of Co<sub>3</sub>O<sub>4</sub> (Co-N<sub>x</sub>/Co<sub>3</sub>O<sub>4</sub>), which exhibited superior catalytic activity. We further fixed the highly efficient Co-N<sub>x</sub>/Co<sub>3</sub>O<sub>4</sub> onto three kinds of organic membranes and one kind of inorganic ceramic membrane installing with the residual PMS treatment device to investigate its catalytic stability and sustainability. Results indicated that the inorganic ceramic membrane (CM) can achieve high water flux of 710 L m<sup>-2</sup> h<sup>-1</sup>, and the similar water flux can be achieved by Co-N<sub>x</sub>/Co<sub>3</sub>O<sub>4</sub>/CM even without the pressure extraction. We also employed the Co-N<sub>x</sub>/Co<sub>3</sub>O<sub>4</sub>/CM system to the wastewater secondary effluent, and the pollutant in complicated secondary effluent could be highly removed by the Co-N<sub>x</sub>/Co<sub>3</sub>O<sub>4</sub>/CM system. This paper provides a new point of view for the application of metal-based catalysts with M-N<sub>x</sub> coordination in catalytic reaction device.

© 2025 Published by Elsevier B.V. on behalf of Chinese Chemical Society and Institute of Materia Medica, Chinese Academy of Medical Sciences.

All kinds of emerging pollutants in water come from various supplies in production and life, such as drugs, skin care products, and various additives [1-4]. These emerging pollutants have a variety of potential effects on people and the environment. However, the traditional treatment technology is difficult to achieve efficient removal of new pollutants, because the emerging pollutants have the characteristics of low concentration and hard to degradation [5-8]. In recent decades, advanced oxidation technologies based on various oxidants (such as perhydrogen peroxide, persulfate, ozone, peracetic acid) have received increasing attentions, because various active substances produced after the activation of these oxidants can efficiently remove various emerging pollutants [9-12]. In recent decades, the advanced oxidation process based on peroxy sulfate (PMS-AOPs) has received more and more attention in the degradation of refractory organic pollutants in water due to its ability to produce a variety of reactive oxygen species (ROS) and strong oxidation capacity. At present, the use of heterogeneous cat-

alysts (metal oxides, carbon-based catalysts or metal carbon-based composite catalysts) to achieve high efficiency activation of PMS is widely studied, but in practical applications, it still faces challenges such as catalytic stability and recovery of powder catalysts [13-15].

Heterogeneous Fenton reaction treats various organic pollutants in water by generating strong oxidizing free radicals and non-free radicals [16,17]. For traditional fully mixed laboratory systems (e.g., beakers, conical bottles), particles dispersed in water face the following problems: (1) Low mass transfer efficiency leads to residual PMS of the system and reduces the oxidation capacity of heterogeneous Fenton system; (2) ROS generated cannot contact the target pollutants quickly, resulting in self-quenching of free radicals or ineffective oxidation reactions (such as the reaction with water molecules) [18-21]. In order to achieve an efficient heterogeneous Fenton system, it is still necessary to improve the reactor operation modules. Many scholars have proposed the concept of membrane confined effect in collaboration with radical/nonradical surface reactions to strengthen the mass transfer process of the system, and developed an advanced oxidized water purification system with high efficiency, high selectivity and high reaction metrology effi-

\* Corresponding authors.

E-mail addresses: [lizhihao050@163.com](mailto:lizhihao050@163.com) (Z. Li), [honw@163.com](mailto:honw@163.com) (W. Hong), [xuxing@sdu.edu.cn](mailto:xuxing@sdu.edu.cn) (X. Xu).

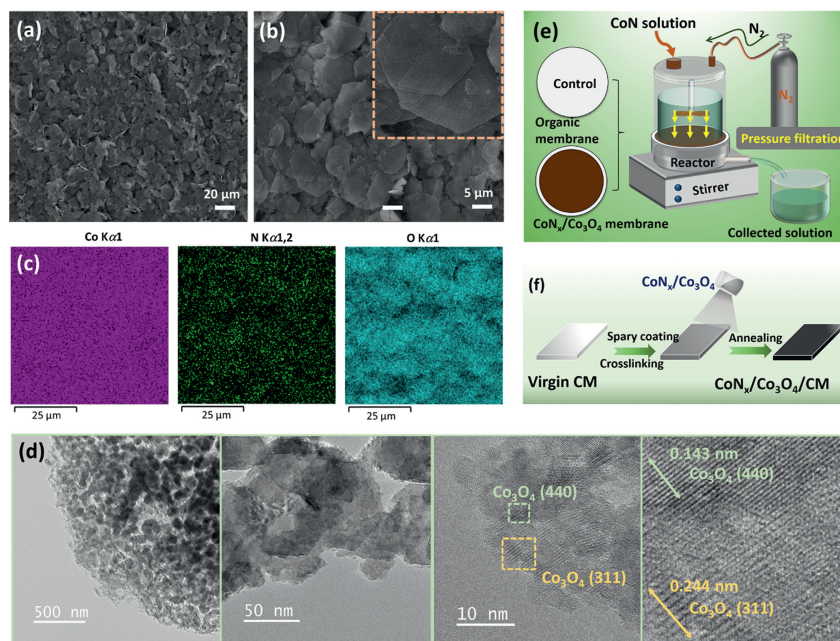


**Fig. 1.** (a) SEM of  $\text{Co-N}_x/\text{Co}_3\text{O}_4$  at (a)  $20\ \mu\text{m}$ , and (b)  $5\ \mu\text{m}$ . (c) SEM mappings of  $\text{Co-N}_x/\text{Co}_3\text{O}_4$ . (d) TEM images of  $\text{Co-N}_x/\text{Co}_3\text{O}_4$  as well as the specific crystal lattices of  $\text{Co}_3\text{O}_4$ . (e) Fabrication procedures for  $\text{Co-N}_x/\text{Co}_3\text{O}_4/\text{PEM}$ ,  $\text{Co-N}_x/\text{Co}_3\text{O}_4/\text{RC}$ , and  $\text{Co-N}_x/\text{Co}_3\text{O}_4/\text{PTFE}$  membranes. (f) Fabrication procedures for  $\text{Co-N}_x/\text{Co}_3\text{O}_4/\text{CM}$  via airbrush spraying routine.

ciency, and carried out systematic research on reaction unit design and application strengthening [22–24]. According to different catalyst types (carbon, metal oxides, and metal/carbon hybrids), the membrane catalytic reaction unit with stable catalyst load and high reaction activity was constructed by introducing the strategies of “self-support” and “polymerization-coating” [21,25,26]. Related studies have solved the problem of low efficiency of lab-scale advanced oxidation technology, and extended the engineering application potential of advanced oxidation water purification technology dominated by free radicals/nonradical pathways [1–3,27–31]. However, there are few systematic studies on multiple catalytic membranes to investigate the water fluxes and degradation performances of different membranes. This is also the focus of this study.

In this work, a cobalt-nitrogen doped cobalt-trioxide catalyst ( $\text{Co-N}_x/\text{Co}_3\text{O}_4$ ) was designed and fabricated by the simple one-step calcination. The structure and composition characteristics of  $\text{Co-N}_x/\text{Co}_3\text{O}_4$  catalyst was analyzed. The catalyst was loaded on the surface of four kinds of inorganic and organic membrane materials (proton exchange membrane (PEM), polytetrafluoroethylene (PTFE), and regenerated cellulose (RC), ceramic membrane (CM)) to investigate the continuous degradation performances of antibiotics in the real environmental conditions.

The  $\text{Co-N}_x$  coordinated  $\text{Co}_3\text{O}_4$  ( $\text{Co-N}_x/\text{Co}_3\text{O}_4$ ) was prepared under ammonia atmosphere. The scanning electron microscopy (SEM) images of  $\text{Co-N}_x/\text{Co}_3\text{O}_4$  displayed that the as-prepared catalyst was formed via stacking the ultra-thin nanosheets (Figs. 1a and b). The distribution of element obtained from the SEM results indicated that the nitrogen derived from ammonia has been introduced into the  $\text{Co}_3\text{O}_4$  (Fig. 1c and Fig. S1 in Supporting information). The atomic force microscopy (AFM) result further confirmed the structure of  $\text{Co-N}_x/\text{Co}_3\text{O}_4$  in the form of nanosheet (Fig. S2 in Supporting information). Transmission electron microscope (TEM) of the  $\text{Co-N}_x/\text{Co}_3\text{O}_4$  showed that the size of  $\text{Co-N}_x/\text{Co}_3\text{O}_4$  was in the range 50–100 nm (Fig. 1d). In addition, the specific crystal lattices of  $\text{Co}_3\text{O}_4$  can also be observed in the  $\text{Co-N}_x/\text{Co}_3\text{O}_4$  nanosheet based on the TEM image. For example, planes of  $\text{Co}_3\text{O}_4$  (440) and (311) showed the specific crystal lattices at 0.143 and

0.244 nm [18,32], respectively (Fig. 1d and Fig. S3 in Supporting information).

The degradation performances of  $\text{Co-N}_x/\text{Co}_3\text{O}_4$  towards different pollutants were shown in Fig. S4 (Supporting information). Results indicated that the  $\text{Co-N}_x/\text{Co}_3\text{O}_4$  could 100% degrade the paracetamol (PCM) and bisphenol-A (BPA) via PMS activation, which exhibited the ultrafast degradation activity of  $\text{Co-N}_x/\text{Co}_3\text{O}_4$ . The electron paramagnetic resonance (EPR) detection indicated that the radical species could be generated and contribute to degradation reaction (Fig. S5 in Supporting information). In addition, open circuit potential of  $\text{Co-N}_x/\text{Co}_3\text{O}_4$  confirmed that there are  $\text{Co-N}_x/\text{Co}_3\text{O}_4+\text{PMS}^*$  in the catalytic system [20,33–38], and the addition of pollutants would result in a sharp decrease in the potential of  $\text{Co-N}_x/\text{Co}_3\text{O}_4$  electrode (Fig. S6 in Supporting information). In contrast, there was no decrease in the potential of  $\text{Co}_3\text{O}_4$  electrode. It was known that electron-transfer process (ETP) can be triggered via the metal-nitrogen coordinated structures [36]. As a result, two major oxidation pathways (radical oxidation, and ETP oxidation) towards different pollutants can be triggered in the  $\text{Co-N}_x/\text{Co}_3\text{O}_4/\text{PMS}$  system, which guaranteed the high-effective degradation activity of  $\text{Co-N}_x/\text{Co}_3\text{O}_4$ .

Four kinds of membrane materials, including the organic materials (PEM, PTFE, and RC) and inorganic CM were selected for depositing the resulting catalyst to form the catalytic membranes ( $\text{Co-N}_x/\text{Co}_3\text{O}_4/\text{PEM}$ ,  $\text{Co-N}_x/\text{Co}_3\text{O}_4/\text{PTFE}$ ,  $\text{Co-N}_x/\text{Co}_3\text{O}_4/\text{RC}$ , and  $\text{Co-N}_x/\text{Co}_3\text{O}_4/\text{CM}$ ). Their fabrication procedures were shown in Figs. 1e and f, which showed two different preparation routines. The  $\text{Co-N}_x/\text{Co}_3\text{O}_4/\text{PEM}$ ,  $\text{Co-N}_x/\text{Co}_3\text{O}_4/\text{PTFE}$ , and  $\text{Co-N}_x/\text{Co}_3\text{O}_4/\text{RC}$  membranes were fabricated via vacuum filtration of the as-prepared  $\text{Co-N}_x/\text{Co}_3\text{O}_4$  catalyst onto the 7 cm-shaped PEM, PTFE, and RC membranes. Their actual images were given in Fig. S7 (Supporting information). In contrast, the fabrication of  $\text{Co-N}_x/\text{Co}_3\text{O}_4/\text{CM}$  was based on the airbrush spraying routine via spraying the  $\text{Co-N}_x/\text{Co}_3\text{O}_4$  inks onto the CMs [36,39], as shown in Fig. S8 (Supporting information).

The SEM cross section images of the four catalytic membranes were shown in Fig. 2 and Fig. S9 (Supporting information). The  $\text{Co-N}_x/\text{Co}_3\text{O}_4/\text{PEM}$  displayed two hierarchies with the thickness of deposited  $\text{Co-N}_x/\text{Co}_3\text{O}_4$  layer approximately  $60\ \mu\text{m}$  (Fig. 2a).

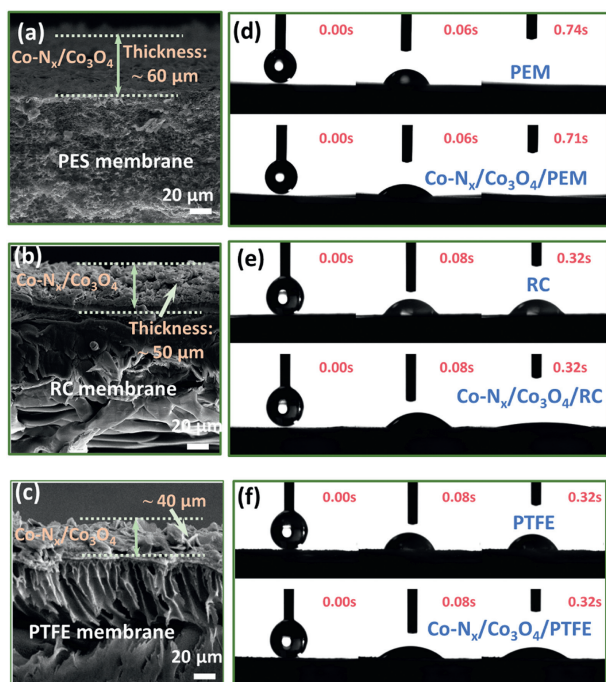


**Fig. 2.** Cross section SEM images of (a) Co-N<sub>x</sub>/Co<sub>3</sub>O<sub>4</sub>/PEM, (b) Co-N<sub>x</sub>/Co<sub>3</sub>O<sub>4</sub>/RC, (c) Co-N<sub>x</sub>/Co<sub>3</sub>O<sub>4</sub>/PTFE. The contact angles of (d) bare PEM membrane and Co-N<sub>x</sub>/Co<sub>3</sub>O<sub>4</sub>/PEM membrane, (e) bare RC membrane and Co-N<sub>x</sub>/Co<sub>3</sub>O<sub>4</sub>/RC membrane, (f) bare PTFE membrane and Co-N<sub>x</sub>/Co<sub>3</sub>O<sub>4</sub>/PTFE membrane.

Similarly, the steady Co-N<sub>x</sub>/Co<sub>3</sub>O<sub>4</sub> layers can be deposited on the PTFE, RC, and CM with the similar thicknesses of 60, 40, and 50 μm, respectively (Figs. 2b and c). As a result, all the four catalytic membranes (including Co-N<sub>x</sub>/Co<sub>3</sub>O<sub>4</sub>/PEM, Co-N<sub>x</sub>/Co<sub>3</sub>O<sub>4</sub>/PTFE, Co-N<sub>x</sub>/Co<sub>3</sub>O<sub>4</sub>/RC, and Co-N<sub>x</sub>/Co<sub>3</sub>O<sub>4</sub>/CM) could provide sufficient reactive sites for oxidizing the pollutants *via* continuous influent flows. The hydrophilicity properties of various catalytic membranes were determined by contact angle experiments [39]. The contact angle results exhibited that depositing the Co-N<sub>x</sub>/Co<sub>3</sub>O<sub>4</sub> onto the organic membranes (PEM, PTFE, and RC) required 0.32–0.74 s for water assimilation (Figs. 2d–f). In contrast, the complete water assimilation of Co-N<sub>x</sub>/Co<sub>3</sub>O<sub>4</sub>/CMs could be achieved within 0.03 s (Fig. S9b). In addition, the Co-N<sub>x</sub>/Co<sub>3</sub>O<sub>4</sub> deposited membranes exhibited similar or even higher hydrophilicity properties as compared with those of bare membranes; this might be attributed to the high populations of oxygen-based groups on these Co-N<sub>x</sub>/Co<sub>3</sub>O<sub>4</sub> deposited mem-

branes, which would accelerate the formation of hydrogen bonds with water molecules and facilitate the water assimilation on the membrane surfaces [36,39].

In addition, the coating of Co-N<sub>x</sub>/Co<sub>3</sub>O<sub>4</sub> onto different membranes showed significantly different flux changes. As shown in Figs. 3a and b, the water flux of original CR was very low (<30 L m<sup>-2</sup> h<sup>-1</sup>), and the Co-N<sub>x</sub>/Co<sub>3</sub>O<sub>4</sub>/CR was even lower than 10 L m<sup>-2</sup> h<sup>-1</sup> (pressure extraction also cannot improve the water flux of Co-N<sub>x</sub>/Co<sub>3</sub>O<sub>4</sub>/CR). As for the original PTFE and Co-N<sub>x</sub>/Co<sub>3</sub>O<sub>4</sub>/PTFE, very low water fluxes were obtained without the pressure extraction (Figs. 3c and d), while the water flux of Co-N<sub>x</sub>/Co<sub>3</sub>O<sub>4</sub>/PTFE can be significantly improved to 820 L m<sup>-2</sup> h<sup>-1</sup> at 0.4 MPa of pressure extraction. The Co-N<sub>x</sub>/Co<sub>3</sub>O<sub>4</sub>/PES could achieve the similar water flux as compared with that of original PES at 0.02 MPa of pressure extraction (Figs. 3e and f). Basically, a certain pressure extraction was required for Co-N<sub>x</sub>/Co<sub>3</sub>O<sub>4</sub> deposited organic membranes (Co-N<sub>x</sub>/Co<sub>3</sub>O<sub>4</sub>/CR, Co-N<sub>x</sub>/Co<sub>3</sub>O<sub>4</sub>/PTFE, and Co-N<sub>x</sub>/Co<sub>3</sub>O<sub>4</sub>/RC). In contrast, the inorganic CM can achieve high water flux of 710 L m<sup>-2</sup> h<sup>-1</sup>, and the similar water flux can be achieved by Co-N<sub>x</sub>/Co<sub>3</sub>O<sub>4</sub>/CM even without the pressure extraction (Figs. 3g and h). This result indicated that the inorganic CM can be more suitable for depositing the Co-N<sub>x</sub>/Co<sub>3</sub>O<sub>4</sub> for continuous Fenton-like reactions.

The Co-N<sub>x</sub>/Co<sub>3</sub>O<sub>4</sub>/CM was then used for the continuous catalytic oxidation of various pollutants in actual Fenton-like system, as shown in Fig. 4a. A residual PMS consumption device (inner diameter of 8 cm and length of 30 cm) filled with Fe<sub>3</sub>O<sub>4</sub> was also equipped. The Fe<sub>3</sub>O<sub>4</sub> filled device could effectively consume the residual PMS in the wastewater secondary effluent, and no PMS can be detected in the effluent after the treatment of the Co-N<sub>x</sub>/Co<sub>3</sub>O<sub>4</sub>/CM system (Fig. 4b). The Co-N<sub>x</sub>/Co<sub>3</sub>O<sub>4</sub>/CM system showed that >98.8% of a series of pollutants (*e.g.*, PCM, BPA, TC, CP) could be stably removed with the continuous flow (20 L) into the catalytic system (Fig. S10 in Supporting information). We also employed the Co-N<sub>x</sub>/Co<sub>3</sub>O<sub>4</sub>/CM system to the wastewater secondary effluent (Zibo Lvhuang wastewater treating plant), and the pollutant in complicated secondary effluent could be highly removed by the Co-N<sub>x</sub>/Co<sub>3</sub>O<sub>4</sub>/CM system (Fig. 4c). These results indicated that the Co-N<sub>x</sub>/Co<sub>3</sub>O<sub>4</sub>/CM could efficiently degrade the pollutants in complex environmental conditions, which exhibited promising application perspectives [21].

The SEM cross section image of used Co-N<sub>x</sub>/Co<sub>3</sub>O<sub>4</sub>/CM after actual Fenton-like reaction was determined, which showed that the thickness of the Co-N<sub>x</sub>/Co<sub>3</sub>O<sub>4</sub> was almost the same as that in original Co-N<sub>x</sub>/Co<sub>3</sub>O<sub>4</sub>/CM (Fig. 5a). This result exhibited the high stability of the Co-N<sub>x</sub>/Co<sub>3</sub>O<sub>4</sub>/CM system. Basically, the Co-N<sub>x</sub>/Co<sub>3</sub>O<sub>4</sub>/CM system could trigger two major oxidation pathways

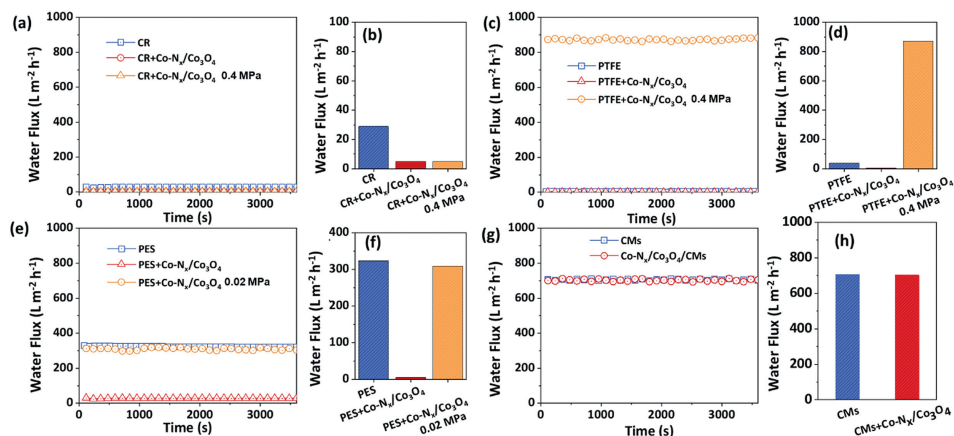


**Fig. 3.** Fluxes of (a, b) Co-N<sub>x</sub>/Co<sub>3</sub>O<sub>4</sub>/CR, (c, d) Co-N<sub>x</sub>/Co<sub>3</sub>O<sub>4</sub>/PTFE, (e, f) Co-N<sub>x</sub>/Co<sub>3</sub>O<sub>4</sub>/PES and (g, h) Co-N<sub>x</sub>/Co<sub>3</sub>O<sub>4</sub>/CM membranes.

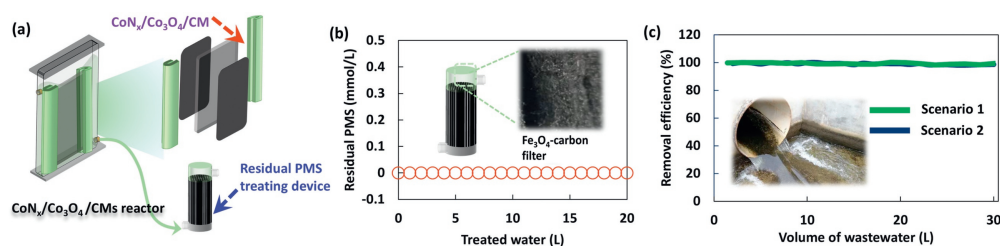


**Fig. 4.** (a) Scheme of the Co-N<sub>x</sub>/Co<sub>3</sub>O<sub>4</sub>/CM equipped with residual PMS consumption device. (b) Residual PMS in the effluent after treatment. (c) Degradation of TC in secondary effluent via Co-N<sub>x</sub>/Co<sub>3</sub>O<sub>4</sub>/CM/PMS system (Pollutant concentrations in feeding solution: 0.25 mg/L).

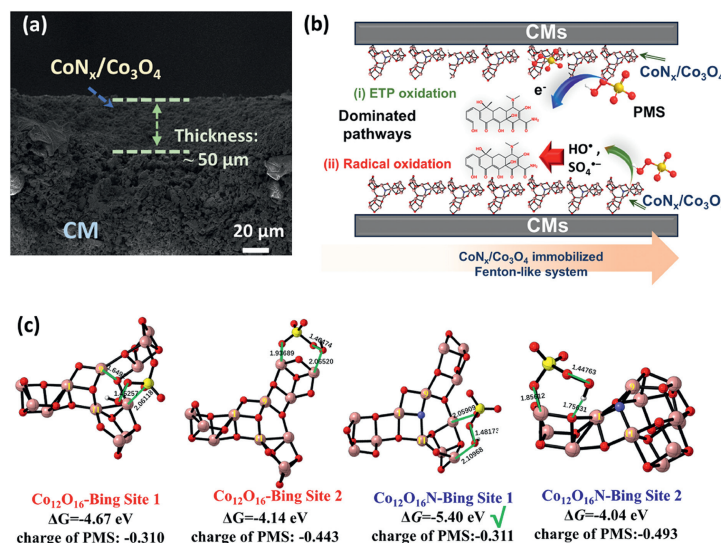


**Fig. 5.** (a) SEM cross section image of used Co-N<sub>x</sub>/Co<sub>3</sub>O<sub>4</sub>/CM. (b) Degradation mechanism of Co-N<sub>x</sub>/Co<sub>3</sub>O<sub>4</sub>/CM towards pollutants via PMS activation. (c) Multiple adsorption models for PMS by Co<sub>3</sub>O<sub>4</sub> and Co-N<sub>x</sub>/Co<sub>3</sub>O<sub>4</sub>.

(radical oxidation, and ETP oxidation) towards different pollutants as obtained from the EPR and GOS systems [40], which guaranteed the high effective and stable degradation activity in the Co-N<sub>x</sub>/Co<sub>3</sub>O<sub>4</sub>/CM system (Fig. 5b). DFT calculation exhibited multiple adsorption models for PMS by Co<sub>3</sub>O<sub>4</sub> and Co-N<sub>x</sub>/Co<sub>3</sub>O<sub>4</sub> (Fig. 5c). Results also confirmed that the Co-N<sub>x</sub>/Co<sub>3</sub>O<sub>4</sub> could exhibit the optimal gibbs free energy (−5.40 eV) as well as the charge of PMS (−0.311), which would facilitate the multiple oxidation pathways in the Co-N<sub>x</sub>/Co<sub>3</sub>O<sub>4</sub>/CM system via activating PMS [40,41], as shown in Fig. 5c.

In summary, developing the eco-friendly, and efficient catalysts for decontaminating the antibiotic wastewaters has become the focus of research in recent years. In this work, Co-N<sub>x</sub> coordinated Co<sub>3</sub>O<sub>4</sub> (Co-N<sub>x</sub>/Co<sub>3</sub>O<sub>4</sub>) was prepared under ammonia atmosphere, which was formed via stacking the ultra-thin nanosheets. The Co-N<sub>x</sub>/Co<sub>3</sub>O<sub>4</sub> could 100% degrade the paracetamol (PCM) and bisphenol-A (BPA) via PMS activation, which exhibited the ultrafast degradation activity of Co-N<sub>x</sub>/Co<sub>3</sub>O<sub>4</sub>. Two major oxidation pathways (radical oxidation, and ETP oxidation) towards different pollutants can be triggered in the Co-N<sub>x</sub>/Co<sub>3</sub>O<sub>4</sub>/PMS system, which guaranteed the high-effective degradation activity of Co-N<sub>x</sub>/Co<sub>3</sub>O<sub>4</sub>. The Co-N<sub>x</sub>/Co<sub>3</sub>O<sub>4</sub> was deposited on the surface of inorganic membranes (PEM, PTFE, and RC membrane) and organic membrane (CM) to investigate the continuous degradation performance of pollutants in the real environmental conditions. Results showed that the membrane permeability can be well controlled in the Co-N<sub>x</sub>/Co<sub>3</sub>O<sub>4</sub>/CM, and stable oxidation activity can be maintained during the continuous catalytic systems. This paper provides some interesting results related to the catalytic modules applied for future large-scale use.

## Declaration of competing interest

The authors declare that they have no known competing financial interests or personal relationships that could have appeared to influence the work reported in this paper.

## CRedit authorship contribution statement

**Qingbai Tian:** Writing – review & editing, Software, Formal analysis, Conceptualization. **BingLiang Yu:** Resources, Methodology. **Zhihao Li:** Resources, Methodology, Formal analysis. **Wei Hong:** Validation, Data curation, Conceptualization. **Qian Li:** Validation, Supervision, Project administration, Methodology. **Xing Xu:** Writing – review & editing, Writing – original draft, Funding acquisition, Formal analysis, Conceptualization.

## Acknowledgments

The work was supported by National Natural Science Foundation of China (Nos. 52170086, 22308194, U22A20423), Natural Science Foundation of Shandong Province (No. ZR2021ME013), Taishan Scholars Program of Shandong Province (No. tsqn202211012), and Shandong Provincial Excellent Youth (No. ZR2022YQ47). The authors also want to thank Conghua Qi from Shiyanjia Lab (www.shiyanjia.com) for DFT analysis.

## Supplementary materials

Supplementary material associated with this article can be found, in the online version, at doi:10.1016/j.ccl.2024.110322.

## References

- [1] M. Sun, C. Chu, F. Geng, et al., *Environ. Sci. Technol. Lett.* 5 (2018) 186–191.
- [2] Y. Shi, D. Yang, C. Hu, L. Lyu, *Environ. Sci. Ecotechnol.* 20 (2024) 100356.
- [3] S. Zhang, T. Cui, X. Liu, et al., *Water Res* 260 (2024) 121949.
- [4] N. Li, X. He, J. Ye, et al., *J. Hazard. Mater.* 458 (2023) 131926.
- [5] Y. Yang, P. Zhang, K. Hu, et al., *Appl. Catal. B: Environ.* 315 (2022) 121593.
- [6] Q. You, C. Zhang, M. Cao, et al., *Appl. Catal. B: Environ.* 338 (2023) 123025.
- [7] P. Zhou, Y. Yang, W. Ren, et al., *Appl. Catal. B: Environ.* 319 (2022) 121916.
- [8] W. Gao, G. Li, Q. Wang, et al., *Chem. Eng. J.* 464 (2023) 142694.
- [9] C. Chen, M. Yan, Y. Li, et al., *Appl. Catal. B: Environ.* 340 (2024) 123218.
- [10] C. Wang, S. Jia, Y. Zhang, et al., *Appl. Catal. B: Environ.* 270 (2020) 118819.
- [11] L. Lai, H. Zhou, Y. Hong, et al., *Chin. Chem. Lett.* 35 (2024) 108580.
- [12] X. Wang, X. Pu, Y. Yuan, et al., *Chin. Chem. Lett.* 31 (2020) 2634–2640.
- [13] V.C. Mora, J.A. Rosso, D.O. Mártire, M.C. Gonzalez, *Chemosphere* 84 (2011) 1270–1275.
- [14] J. Miao, W. Geng, P.J.J. Alvarez, M. Long, *Environ. Sci. Technol.* 54 (2020) 8473–8481.
- [15] W. Ren, C. Cheng, P. Shao, et al., *Environ. Sci. Technol.* 56 (2022) 78–97.
- [16] Preethi, S.P. Shanmugavel, G. Kumar, et al., *Environ. Pollut.* 341 (2024) 122842.
- [17] W. Cao, Z. Wang, P. Zhang, et al., *Environ. Sci. Ecotechnol.* 57 (2023) 2837–2845.
- [18] X. Pan, S. Mei, W.J. Liu, *Chin. Chem. Lett.* 34 (2023) 108034.
- [19] Y. Wei, J. Miao, J. Ge, et al., *Environ. Sci. Technol.* 56 (2022) 8984–8992.
- [20] M. Yang, Z. Hou, X. Zhang, et al., *Environ. Sci. Technol.* 56 (2022) 11635–11645.
- [21] Y. Zhang, S. Liu, H. Deng, et al., *Chin. Chem. Lett.* 35 (2024) 108666.
- [22] F. Chen, X.T. Huang, C.W. Bai, et al., *Chem. Eng. J.* 481 (2024) 148789.
- [23] T. Liu, S. Xiao, N. Li, et al., *Nat. Commun.* 14 (2023) 2881.
- [24] Chen, Y.J. Sun, X.T. Huang, et al., *P. Natl Acad. Sci. U. S. A.* 121 (2024) e2314396121.
- [25] Y. Chai, H. Dai, X. Duan, et al., *Appl. Catal. B: Environ.* 341 (2024) 123289.
- [26] K. Yin, J. Yang, Y. Li, et al., *Chin. Chem. Lett.* 35 (2024) 109847.
- [27] S. Zhan, H. Zhang, X. Mi, et al., *Environ. Sci. Technol.* 54 (2020) 8333–8343.
- [28] C. Zhang, C. Kong, P.G. Tratnyek, et al., *Environ. Sci. Technol.* 58 (2024) 1378–1389.
- [29] H. Zhou, J. Peng, X. Duan, et al., *Environ. Sci. Technol.* 57 (2023) 3334–3344.
- [30] A. Bhatt, M. Khanchandani, M.S. Rana, S.K. Prajapati, *J. Clean. Prod.* 370 (2022) 133456.
- [31] C. Yu, C. Yan, J. Gu, et al., *J. Clean. Prod.* 427 (2023) 139334.
- [32] J. Zhang, H. Lu, T. Yao, et al., *Chin. Chem. Lett.* 35 (2024) 108450.
- [33] L. Peng, X. Duan, Y. Shang, et al., *Appl. Catal. B: Environ.* 287 (2021) 119963.
- [34] K. Yin, Y. Shang, D. Chen, et al., *Appl. Catal. B: Environ.* 338 (2023) 123029.
- [35] K. Yin, R. Wu, Y. Shang, et al., *Appl. Catal. B: Environ.* 329 (2023) 122558.
- [36] J. Guo, Y. Wang, Y. Shang, et al., *P. Natl Acad. Sci. U. S. A.* 121 (2024) e2313387121.
- [37] S. Luo, Z. Wei, D.D. Dlonysiou, et al., *Chem. Eng. J.* 327 (2017) 1056–1065.
- [38] J. Ma, L. Xu, C. Shen, et al., *Environ. Sci. Technol.* 52 (2018) 3608–3614.
- [39] K. Yin, L. Peng, D. Chen, et al., *Appl. Catal. B: Environ.* 336 (2023) 122951.
- [40] Q. Zeng, Y. Wen, X. Duan, et al., *Appl. Catal. B: Environ. Energy.* 346 (2024) 123752.
- [41] J. Mao, K. Yin, Y. Zhang, et al., *Appl. Catal. B: Environ.* 342 (2024) 123428.